Available online at www.sciencedirect.com

ScienceDirect

Ceramics International 40 (2014) 2863–2868

CERAMICS INTERNATIONAL

www.elsevier.com/locate/ceramint

Nanoceria: Gum mediated synthesis and *in vitro* viability assay

Majid Darroudi[a,b,*], Mina Sarani[c], Reza Kazemi Oskuee[b,d], Ali Khorsand Zak[e], Mohammad Sadegh Amiri[f]

[a]*Nuclear Medicine Research Center, School of Medicine, Mashhad University of Medical Sciences, Mashhad, Iran*
[b]*Department of Modern Sciences and Technologies, School of Medicine, Mashhad University of Medical Sciences, Mashhad, Iran*
[c]*Zabol Medicinal Plants Research Center, Zabol University of Medical Sciences, Zabol, Iran*
[d]*Targeted Drug Delivery Research Center, Mashhad University of Medical Sciences, Mashhad, Iran*
[e]*Nanotechnology Laboratory, Esfarayen University, North Khorasan, Iran*
[f]*Department of Biology, Payame Noor University, Tehran, Iran*

Received 27 September 2013; received in revised form 30 September 2013; accepted 6 October 2013
Available online 12 October 2013

Abstract

Green and Biological synthetic methods for preparing of different nanoparticles (e.g., metal and metal oxide) using microorganisms, enzymes, and plant extracts have been suggested as a possible low cost and eco-friendly alternative to chemical and physical methods. In this paper, we would like to report the green and biosynthesis of nanoceria particles (NCs), using *gum tragacanth* by both chemical and biological methods. The NCs were synthesized at different calcination temperatures and structural, morphological, and optical properties of the synthesized NCs have been characterized by using UV–vis spectrophotometer, FESEM, PXRD analysis. FESEM images display that the NCs prepared were monodispersed and the average size was ranged from about 20 to 40 nm. *In vitro* viability studies on neuro2A cells, a dose dependent toxicity with non-toxic effect of concentrations below 30 μg/mL is presented. The synthesis of NCs using *gum tragacanth* was found to be comparable to those obtained from conventional reduction methods using hazardous polymers or surfactants.

Keywords: A. Sol–gel processes; B. Electron microscopy; D. CeO_2

1. Introduction

During the past decay, nanoceria (NCs) have been widely studied for its structural, chemical, and physical properties that are significantly different from those of bulk materials [1,2]. Therefore, it has been widely considered in various areas, such as catalysis [3], gas sensors [4], fuel cells [5], hydrogen storage materials [6], optical devices [7], ultraviolet absorbers [8], polishing materials [9], and biomedical science fields [10]. Various preparation methods have been used to obtain dispersed NCs such as hydrothermal [11], pyrolysis [12], precipitation [13], thermo-decomposition [14], sol–gel [15], microwave heating [16], sonochemical [17], W/O microemulsions [18], and mechanochemical [19] methods. However, some of these routes (e.g., sol–gel and precipitation) have occurred in colloidal media (e.g., emulsions or polymers) in order to improve or control chemical or physical properties (e.g., control the particle growth and surface area of the CeO_2-NPs).

Gum tragacanth (GT) is a naturally occurring complex and acidic polysaccharide derived as an exudate from the bark of *Astragalus gummifer* (Fabaceae family) which is a native tree found in western Asia while it is commercially produced in Iran (accounting for ~70% of the supplies) and Turkey [20]. This biopolymer is an arabinogalactan type of natural gum and its structural, physicochemical, compositional, solution, thermal, rheological and emulsifying properties have been well characterized and studied [21,22]. This natural polymer

*Corresponding author at: Nuclear Medicine Research Center, School of Medicine, Mashhad University of Medical Sciences, Mashhad, Iran. Tel.: +98 511 800 2286; fax: +98 511 800 2287.
E-mail addresses: majiddarroudi@gmail.com, darroudim@mums.ac.ir (M. Darroudi).

0272-8842/$ - see front matter © 2013 Elsevier Ltd and Techna Group S.r.l. All rights reserved.
http://dx.doi.org/10.1016/j.ceramint.2013.10.026

consists of a mixture of water-soluble (tragacanthin) and water-swellable (bassorin) polysaccharide fractions [20,23]. In this study, we demonstrate a sol–gel method using GT to synthesize NCs. Cerium nitrate was used as the cerium source at different calcination temperatures and the synthesized samples were characterized using FTIR, FESEM, PXRD, and UV–vis spectroscopy. The main point of this work is introducing synthesis of nanomaterials in plants as a green, eco-friendly, low cost method which can be consequently used as a valuable alternative for large-scale production of metal oxide nanoparticles.

2. Materials and methods

2.1. Materials and reagents

Chemicals compounds which are used in this work were in analytical grade and were used as received without further purification. Cerium (III) nitrate hexahydrate [$Ce(NO_3)_3 \cdot 6H_2O$, Merck] and ammonium hydroxide solution (NH_4OH, 25 vol%; Merck) were used as the starting materials. The GT used in this study was a high quality ribbon type, collected from the stems of *Astragalus verus* that grow in north eastern areas of Iran (Daregaz), and was grounded into fine powder. For the evaluation of neurotoxicity effect, Neuro2A murine neuroblastoma cells (ATCC CCL-131, Manassas, VA, USA) were grown in Dulbecco's modified Eagle's medium (1 g/L glucose, 2 mM glutamine), supplemented with 10% FBS, streptomycin at 100 μg/ml, and penicillin at 100 U/ml while all cells were incubated at 37 °C in a humidified 5% CO_2 atmosphere.

2.2. Synthesis of CNs

To prepare the CNs, 0.2 g of GT powder was dissolved in 20 ml of distilled water and was stirred for 10 min at 40 °C to achieve a clear GT solution; meanwhile, the required amount of 0.5 M cerium nitrate solution was added to the GT solution slowly under vigorously stirring. The resulting solution was stirred for 30 min, and an excess amount of 1 M of ammonia solution was added in a drop-wise manner until the solution pH reached 10. Initially, the solution color changed to light yellow and as the ammonia concentration increased, it completely turned to yellow. The solution was allowed to be stirred one more hour. The final yellow-colored precipitate was centrifuged and washed several times with acetone and water to make it clear of nitrate, ammonia, and organic impurities and was subsequently dried at 80 °C for 12 h and the sample was stored in a vacuum desiccator for further studies. The obtained sample was divided into 4 parts that were heat treated at 120 °C (NCs1), 200 °C (NCs2), 400 °C (NCs 3), and 600 °C (NCs 4) for 2 h each and characterized.

2.3. Characterization of NCs

The prepared NCs were characterized by powder X-ray diffraction (PXRD, Philips, X'pert, Cu K_α), UV–vis spectrophotometry (UV–vis, Evolution 300® Thermo Fisher Scientific), field emission scanning electron microscopy (FESEM, Carl Zeiss Supra 55VP), and FTIR (ST-IR\ST-SIR spectrometer).

2.4. Evaluation of neurotoxicity effect

The cytotoxicity of nanoparticles was evaluated by the method using 3-(4,5-dimethylthiazol-2-yl)-2,5-diphenylte-trazolium bromide (MTT) assay [24]. Briefly, neuro2A cells were seeded at a density of 1×10^4 cells per well in 96-well plates and incubated for 24 h. Thereafter, the cells were treated with various concentrations of nanoparticles in the presence of 10% FBS. The calcined ZnO-NPs at 600 °C were suspended in a stock solution at 5 μg/ml in a solution of dimethyl sulfoxide (DMSO)/double distilled water. After 24 h of incubation, 20 μl of 5 mg/ml MTT in the PBS buffer was added to each well, and had the cells further incubated for 4 h at 37 °C. The medium containing unreacted dye was discarded, and 100 μl of DMSO was added to dissolve the formazan crystal formed by live cells. Optical absorbance was measured at 590 nm (reference wavelength 630 nm) using a microplate reader (Statfax-2100, Awareness Technology, USA), and cell viability was expressed as a percent relative to untreated control cells. Also values of metabolic activities are presented as mean ± SD of triplicates.

3. Results and discussion

When the hydrocolloid GT is mixed and stirred with distilled water, only the soluble fraction (tragacanthin or tragacanthic acid) dissolves to give a colloidal hydrosol whereas the insoluble fraction (bassorin) swells to a gel form [25,26]. The TG has a molecular weight of about 840 kDa, calculated by Svedberg's method and formula and an elongated shape of 450 nm by 1.9 nm, providing a high viscosity [20]. Chemically, tragacanthin is a complex mixture of acidic branched hetero-polysaccharides that contains D-galacturonic acid. The other sugars produced on hydrolysis are D-galactose, L-fucose (6-deoxy-L-galactose), D-xylose, and L-arabinose. Bassorin (arabinogalactan) which appears to be nearly neutral, contained mainly D-galacturonic acid methylester instead of acid units [25,27].

Based on this experiment, a tentative responsible mechanism for the formation of NCs has been proposed and illustrated in Scheme 1. The GT becomes soluble in water when the temperature of the cloudy solution reaches 40 °C and the semi-crystalline structure is lost. After adding the cerium nitrate solution to GT solution, the metal cations are attracted by the oxygen of OH branches. By continuing the heating process to decrease the amount of water, the smaller released molecules from GT start forming a network that holds water, resulting – in an increase – of the mixture's viscosity. The nitrate decomposes to nitrogen dioxide and oxygen during the heating process, and will be removed from the compounds [28]. Although the formation of NCs involves several complicated reactions [29], however controlling the nucleation of initial precipitate $Ce(OH)_3$, will mainly determine the properties of the final NCs. As the NH_4OH was added into

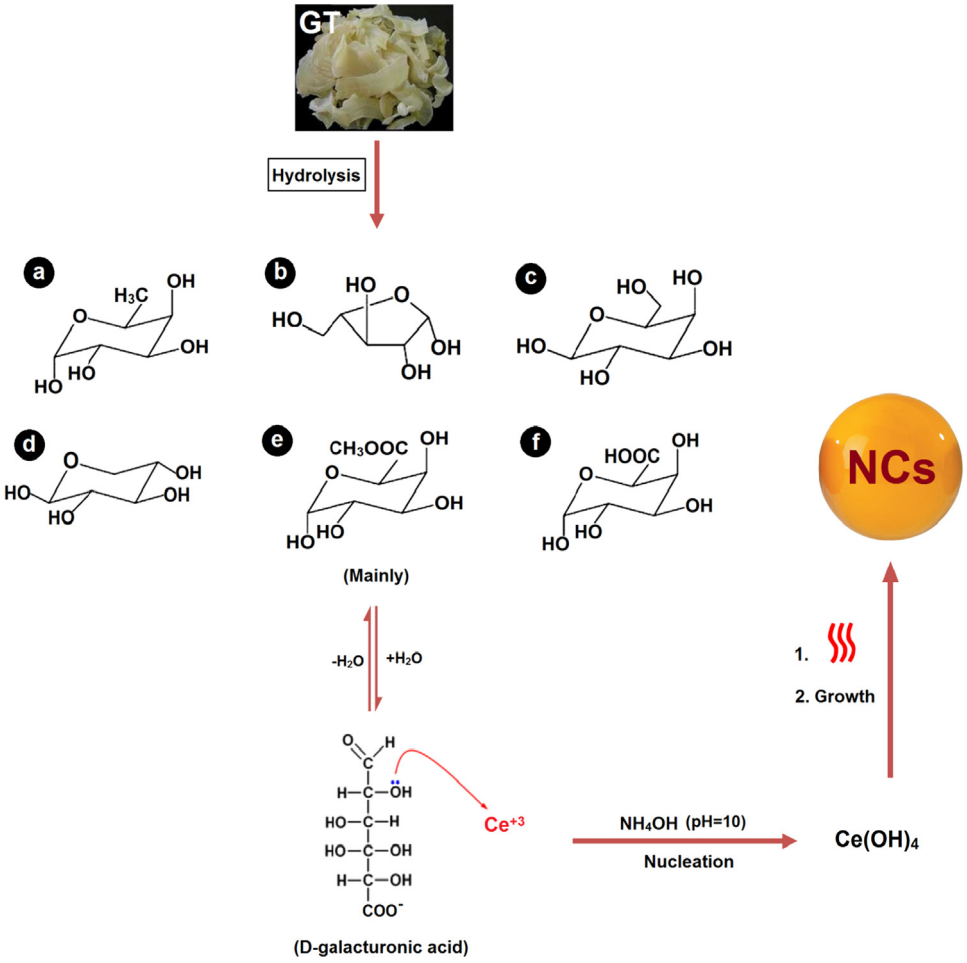

Scheme 1. Schematic plan of formation mechanism of NCs and GT components: (a) α-L-fucose, (b) L-arabinose, (c) β-D-galactose, (d) β-D-xylose, (e) α-D-galacturonic acid methylester, and (f) α-D-galacturonic.

the precursor, $Ce(OH)_3$ precipitate was formed immediately due to extremely low-solubility constant ($K_{sp}=6.3\times10^{-24}$) [30]. Under such a basic condition, high-alkaline environment favored the oxidation of $Ce(OH)_3$ to hydrated Ce(IV) and the color of the initial solution changed from colorless to light yellow. Oxidation of Ce^{3+} to Ce^{4+} in the solution takes place at high pH with subsequent hydrolysis to $Ce(OH)_4$ and precipitation. Hydroxyl ions play an important role in this process and strongly affect the super saturation degree of initial precipitate and oxidation of Ce(III) to Ce(IV) [31]. The subsequent sol–gel procedure and heat treatment afforded enough energy for the complete conversion of $Ce(OH)_4$ nuclei into CeO_2 nuclei via dehydration and the subsequent growth of highly crystallized NCs, which were stabilized by GT molecules and their fractions. The stabilizing effect of TG is the result of the steric repulsion force arising as the gum forms a layer around the cerium hydroxides and finally NCs in solutions. On the other hand, the ability of TG to stabilize NCs may also be due to electrostatic interactions in addition to enhancement of suspension viscosity [32,33].

The typical room temperature UV–vis absorption spectrum of the NCs3 is shown in Fig. 1. The NCs3 were dispersed in water with concentration of 0.1 wt% and afterwards the solution was used to perform the UV–vis measurement. The spectrum revealed a characteristic absorption peak at wavelength of 307 nm for NCs3, which can be assigned to the intrinsic band-gap absorption of nanoceria powders due to the electron transitions from the valence band to the conduction

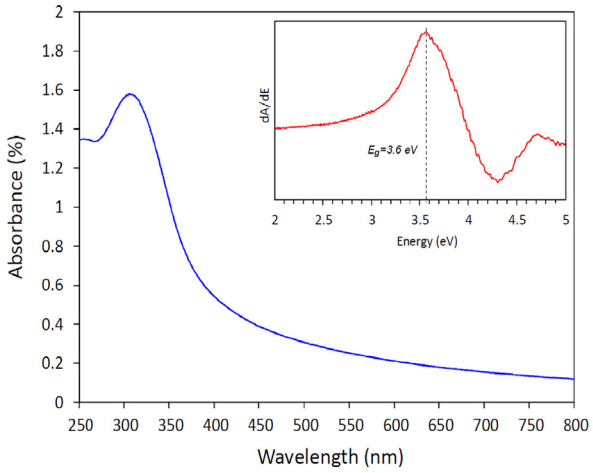

Fig. 1. UV–vis spectrum and band gap estimation (inset) of NCs3.

band. In other words, the absorption of the charge transfer transition from O 2p to Ce 4f in CeO_2 produces the band at approximately 300 nm [34,35]. As shown in Fig. 1, the maximum peak in the absorbance spectrum does not correspond to the true optical band gap of the nanoceria. A common way to obtain the band gap of the materials with a direct band gap from the absorbance spectra is to get the first derivative of the absorbance with respect to the photon energies. The band gap can be estimated from the maximum in the derivative spectrum at the lower energy sides [36,37]. The derivative of the absorbance of the nanoceria shown in the inset of Fig. 1, indicates a band gap of 3.6 eV for the sample.

The NCs is a kind of typical calcium fluoride (CaF_2) structure with space group Fm^3m. Fig. 2 shows the PXRD patterns of the dried and calcined NCs that were synthesized in the GT substrate in different temperatures. The same crystalline structure for all temperatures was observed. All of the detectable Bragg's peaks with Miller indices (111), (200), (220), (311), (222), (400), (331), (420), and (422) can be indexed as the fluorite cubic structure (JCPDS # 00-043-1002). The full width at half maxima for all the peaks of the samples were broader due to the combined effect of small crystal dimension and associated relatively higher crystal lattice strain and defects [38]. The broadening of the PXRD peaks also indicate that the crystallite sizes of obtained NCs are below 50 nm, according to the literature [29] and this result impresses that the size of the obtained samples are small, as confirmed by the FESEM images of NCs3 in different magnifications (Fig. 3). After the as-prepared NCs was calcined in 200 °C, 400 °C, and 600 °C for 2 h, PXRD peaks became sharper with increasing calcination temperatures and FWHM decreased, indicating that the crystallinity of NCs are accelerated by the calcination process. No peaks from possible intermediate phases, such as $Ce(OH)_4$/$Ce(OH)_3$ were detected in PXRD patterns for the prepared NCs in different calcination temperatures, indicating that the final samples were pure. Fig. 3 illustrates the FESEM images of NCs3 in high magnifications. It is evident from the images that obtained NCs were small in size and uniform in shape. The FTIR spectrum of NCs3 is shown in Fig. 4. The spectrum was recorded in the wavenumber range of 400–4000 cm^{-1}. The intense bands at 3234 and 1651 cm^{-1} correspond to the ν (O–H) mode of (H-bonded) water molecules and δ (OH), respectively. The intensive band at 1386 cm^{-1} represents N–O stretch due to the presence of nitrate and the absorption band at wavenumber 551 cm^{-1} represents the Ce–O stretch [39]. The FTIR spectrum of the ceria also exhibits strong broad band ~750 cm^{-1} which is due to the δ (Ce–O–C) mode, in order to confirm the formation of pure ceria [40].

The results of *in vitro* cytotoxicity studies after 24 h of incubation with different concentrations of nanoparticles, ranging from 0 to 125 μg/mL, are shown in Fig. 5. The samples demonstrated no significant toxicity even higher concentrations up to 30 μg/mL which are routinely used in biological applications were well tolerated by Neuro2A cells in the MTT assay. Few studies have investigated the toxicity that is induced by NCs while the results of this study can be useful

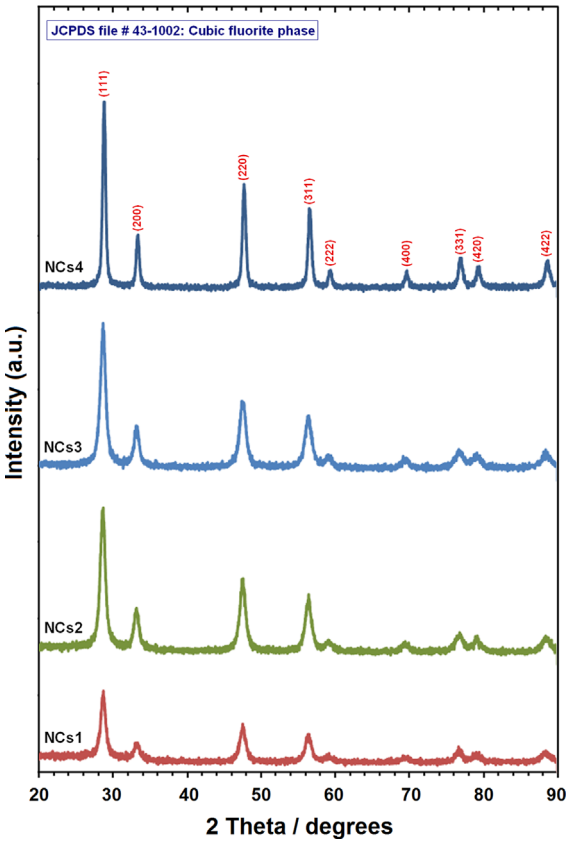

Fig. 2. PXRD patterns of synthesized CNs in different calcination temperatures: NCs1: 120 °C, NCs2: 200 °C, NCs3: 400 °C, and NCs4: 600 °C.

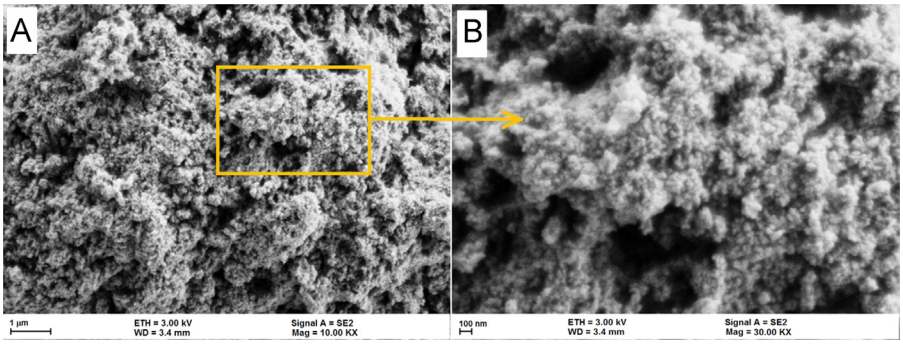

Fig. 3. FESEM images of synthesized NCs3 in different magnifications: (A) × 10,000 and (B) × 30,000.

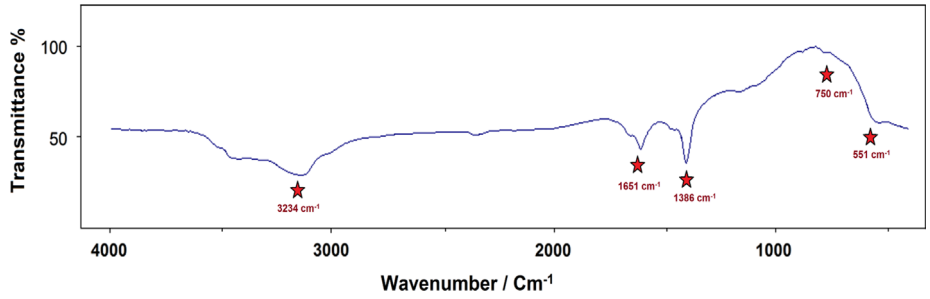

Fig. 4. The FTIR spectrum of NCs3.

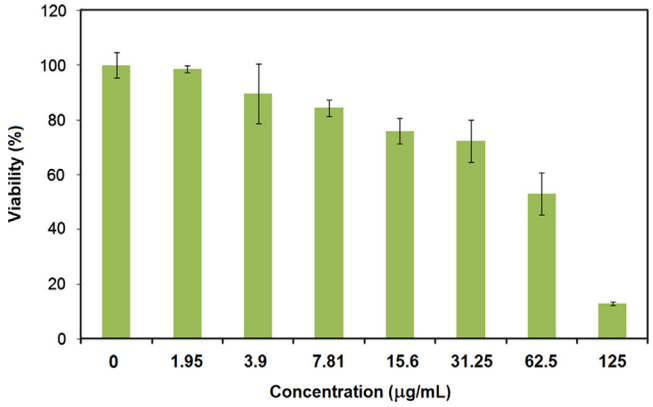

Fig. 5. Cell viability of Neuro2A cells measured by the MTT assay (cells were incubated for 24 h with the indicated concentrations of the NCs3).

for the potential biological applications of nanoceria such as drug delivery studies [41–44].

4. Conclusions

The NCs with narrow size and high homogeneity were synthesized by GT-mediated sol–gel method in aqueous solutions. This method is found to be simple, green, and low cost for large preparations of NCs with the required characteristics. The obtained results suggest that the mean diameter of nanoceria powders was found near below 10 nm, with cubic fluoride structure. The NCs showed a strong and well-defined UV–vis absorption peak at around 300 nm and the direct band gap was found to be 3.6 eV. The NCs exhibited very low cytotoxic effect on Neuro2A cell lines, making it a suitable candidate for various biological applications.

References

[1] M. Darroudi, M. Sarani, R. Kazemi Oskuee, A. Khorsand Zak, H.A. Hosseini, L. Gholami, Green synthesis and evaluation of metabolic activity of starch mediated Nanoceria, Ceram. Int. (2013)http://dx.doi.org/10.1016/j.ceramint.2013.07.116 (in press).

[2] X. Jiao, H. Song, H. Zhao, W. Bai, L. Zhang, Y. Lv, Well-redispersed ceria nanoparticles: promising peroxidase mimetics for H_2O_2 and glucose detection, Anal. Methods 4 (2012) 3261–3267.

[3] Q. Fu, H. Saltsburg, M. Flytzani-Stephanopoulos, Active non-metallic Au and Pt species on ceria-based water–gas shift catalysts, Science 301 (2003) 935–938.

[4] P. Jasinski, T. Suzuki, H.U. Anderson, Nanocrystalline undoped ceria oxygen sensor, Sensors Actuators B 95 (2003) 73–77.

[5] G. Jacobs, L. Williams, U. Graham, D. Sparks, B.H. Davis, Low-temperature water-gas shift: in-situ DRIFTS-reaction study of a Pt/CeO_2 catalyst for fuel cell reformer applications, J. Phys. Chem. B 107 (2003) 10398–10404.

[6] K. Sohlberg, S.T. Pantelides, S.F. Pennycook, Interactions of hydrogen with CeO_2, J. Am. Chem. Soc. 123 (2001) 6609–6611.

[7] F. Goubin, X. Rocquefelte, M.H. Whangbo, Y. Montardi, R. Brec, S. Jobic, Experimental and theoretical characterization of the optical properties of CeO_2, $SrCeO_3$, and Sr_2CeO_4 containing Ce^{4+} (f^0) ions, Chem. Mater. 16 (2004) 662–669.

[8] R.X. Li, S. Yabe, M. Yamashita, S. Momose, S. Yoshida, S. Yin, T. Sato, Synthesis and UV-shielding properties of ZnO- and CaO-doped CeO_2 via soft solution chemical process, Solid State Ionics 151 (2002) 235–241.

[9] D.G. Shchukin, R.A. Caruso, Template synthesis and photocatalytic properties of porous metal oxide spheres formed by nanoparticle infiltration, Chem. Mater. 16 (2004) 2287–2292.

[10] C.W. Younce, K.K. Wang, P.E. Kolattukudy, Hyperglycaemia-induced cardiomyocyte death is mediated via MCP-1 production and induction of a novel zinc-finger protein MCPIP, Cardiovasc. Res. 87 (2010) 665–674.

[11] A.I.Y. Tok, F.Y.C. Boey, Z. Dong, X.L. Sun, Hydrothermal synthesis of CeO_2 nanoparticles, J. Mater. Process. Technol. 190 (2007) 217–222.

[12] J. Hu, Y. Li, X. Zhou, M. Cai, Preparation and characterization of ceria nanoparticles using crystalline hydrate cerium propionate as precursor, Mater. Lett. 61 (2007) 4989–4992.

[13] H.-I. Chen, H.-Y. Chang, Synthesis of nanocrystalline cerium oxide particles by the precipitation method, Ceram. Int. 31 (2005) 795–802.

[14] L. Li, Y. Chen, Preparation of nanometer-scale CeO_2 particles via a complex thermo-decomposition method, Mater. Sci. Eng. A 406 (2005) 180–185.

[15] H.-W. He, X.-Q. Wu, W. Ren, P. Shi, X. Yao, Z.-T. Song, Synthesis of crystalline cerium dioxide hydrosol by a sol–gel method, Ceram. Int. 38 (2012) S501–S504.

[16] M.M. Natile, A. Glisenti, Nanostructured CeO_2 powders by XPS, Surf. Sci. Spectra 13 (2006) 17–31.

[17] J.C. Yu, L. Zhang, J. Lin, Direct sonochemical preparation of high-surface-area nanoporous ceria and ceria–zirconia solid solutions, J. Colloid Interface Sci. 260 (2003) 240–243.

[18] K. Nagy, I. Dékány, Preparation of nanosize cerium oxide particles in W/O microemulsions, Colloids Surf. A Physicochem. Eng. Aspects 345 (2009) 31–40.

[19] T.P. Yadav, O.N. Srivastava, Synthesis of nanocrystalline cerium oxide by high energy ball milling, Ceram. Int. 38 (2012) 5783–5789.

[20] G.O. Phillips, P.A. Williams, Handbook of Hydrocolloids, Woodhead Publishing Limited, Cambridge, 2009.

[21] M.J. Zohuriaan, F. Shokrolahi, Thermal studies on natural and modified gums, Polym. Test. 23 (2004) 575–579.

[22] F. Chenlo, R. Moreira, C. Silva, Rheological behavior of aqueous systems of tragacanth and guar gums with storage time, J. Food Eng. 96 (2010) 107–113.

[23] N. Gralen, M. Karrholm, The physicochemical properties of solutions of gum tragacanth, J. Colloid Sci. 5 (1950) 21–36.

[24] T. Mosmann, Rapid colorimetric assay for cellular growth and survival: application to proliferation and cytotoxicity assays, J. Immunol. Methods 65 (1983) 55–63.
[25] L. Whistler, J.N. Bemiller, Industrial Gums (Polysaccharides and Their Derivatives), Academic Press, New York, 1973.
[26] R.L. Davidson, Handbook of Water Soluble Gums and Resins, McGraw-Hill, New York, 1980.
[27] J.R. Daniel, R.L. Whistler, A.C.J. Voragen, in: B. Elvers, S. Hawkins, W. Russey (Eds.), Ullmann's Encyclopedia of Industrial Chemistry, vol. A25, VCH, Weinheim, 1994, pp. 1–62.
[29] A. Khorsand Zak, W.H.A. Majid, M.R. Mahmoudian, M. Darroudi, R. Yousefi, Starch-stabilized synthesis of ZnO nanopowders at low temperature and optical properties study, Adv. Powder Technol. 24 (2013) 618–624.
[30] X.D. Zhou, W. Huebner, H.U. Anderson, Processing of nanometer-scale CeO_2 particles, Chem. Mater. 15 (2003) 378–382.
[31] O. Söhnel, J. Garside, Precipitation, Butterworth-Heinemann, Boston, 1992.
[32] H.-I. Chen, H.-Y. Chang, Homogeneous precipitation of cerium dioxide nanoparticles in alcohol/water mixed solvents, Colloids Surf. A Physicochem. Eng. Aspects 242 (2004) 61–69.
[33] A. Yokoyama, K.R. Srinivasan, H.S. Folger, Stabilization mechanism of colloidal suspensions by gum tragacanth: the influence of pH on stability, J. Colloid Interface Sci. 126 (1988) 141–149.
[34] E. Rezvani, G. Schleining, G. Sumen, A.R. Taherian, Assessment of physical and mechanical properties of orange oil-in-water beverage emulsions using response surface methodology, LWT-Food Sci. Technol. 48 (2012) 82–88.
[35] Z.C. Orel, B. Orel, Optical properties of pure CeO_2 and mixed CeO_2/SnO_2 thin film coatings, Phys. Status Solidi B 186 (1994) K33–K36.
[36] M.I. Zaki, G.A.M. Hussein, S.A.A. Mansour, H.M. Ismail, G.A. H. Mekhemer, Ceria on silica and alumina catalysts: dispersion and surface acid–base properties as probed by X-ray diffractometry, UV–vis diffuse reflectance and in situ IR absorption studies, Colloids Surf. A Physicochem. Eng. Aspects 127 (1997) 47–56.
[37] A.K. Zak, R. Razali, W.H.A. Majid, M. Darroudi, Synthesis and characterization of a narrow size distribution of zinc oxide nanoparticles, Int. J. Nanomed. 6 (2011) 1399–1403.
[38] S. Deshpande, S. Patil, S. Kuchibhatla, S. Seal, Size dependency variation in lattice parameter and valency states in nanocrystalline cerium oxide, Appl. Phys. Lett. 87 (2005) 133113.
[39] A.A. Ansari, P.R. Solanki, B.D. Malhotra, Hydrogen peroxide sensor based on HRP immobilized nanostructured cerium oxide film, J. Biotechnol. 142 (2009) 179–184.
[40] M.L. Dos Santos, R.C. Lima, C.S. Riccardi, R.L. Tranquilin, P.R. Bueno, J.A. Varela, E. Longo, Preparation and characterization of ceria nanospheres by microwave-hydrothermal method, Mater. Lett. 62 (2008) 4509–4511.
[41] B. Djuričić, S. Pickering, Nanostructured cerium oxide: preparation and properties of weakly-agglomerated powders, J. Eur. Ceram. Soc. 19 (1999) 1925–1934.
[42] M. Darroudi, M. Hakimi, M. Sarani, R. Kazemi Oskuee, A. Khorsand Zak, L. Gholami, Ceram. Int. 39 (2013) 6917–6921.
[43] I. Celardo, E. Traversa, L. Ghibelli, J. Exp. Ther. Oncol. 9 (2011) 47–51.
[44] I. Celardo, J.Z. Pedersen, E. Traversa, L. Ghibelli, Nanoscale 3 (2011) 1411–1420.